

Stereo object matching for mobile robot path planning using artificial fish algorithms

Andi Besse Firdausiah Mansur

Faculty of Computing and Information Technology in Rabigh, King Abdulaziz University, Jeddah, Saudi Arabia

Article Info

Article history:

Received Oct 29, 2023

Revised Dec 30, 2023

Accepted Jan 3, 2024

Keywords:

AdaBoost

Artificial fish

Path planning

Recognition

Stereo object matching

ABSTRACT

The popularity of robots is on the rise, not only in industrial settings but increasingly in daily venues such as airports. Recently, some organizations have carried out experiments utilizing robots specifically created to improve airport hygiene, security, and passengers' overall satisfaction. Furthermore, the utilization of the artificial fish (AFs) algorithm in path planning for mobile robots yielded exceptional outcomes. The robot can replicate the prey behavior of the AFs algorithm, as evidenced by the prevalence of pos one in the simulation. The robot exhibits another behavior, which is the subsequent behavior. The behavior of the AFs algorithm is influenced by the available food sources. Simultaneously, mobile robots are influenced by the stimulation of their neighboring responses. Afterwards, the three primary classifiers are employed to perform stereo-object matching on different objects. The recognition rate achieved by the AdaBoost classifier is promising, with an accuracy rate of 92.4%. This result shows excellent potential for improving the path planning of mobile robots equipped with visual surveillance systems for their surroundings.

This is an open access article under the [CC BY-SA](https://creativecommons.org/licenses/by-sa/4.0/) license.



Corresponding Author:

Andi Besse Firdausiah Mansur

Faculty of Computing and Information Technology in Rabigh, King Abdulaziz University

Jeddah, Saudi Arabia

Email: abmansur@kau.edu.sa

1. INTRODUCTION

The utilization of robots holds significant significance in the daily lives of individuals. Certain robots are employed for the purpose of educating children in a manner that is both engaging and enjoyable [1]. Moreover, path planning is a prominent area of research in the field of mobile robotics, with significant applications in industries, healthcare, and public services. The topics of interest include photogrammetry, 3D reconstruction, and autonomous driving [2]–[6]. The primary objective of path planning research topics is to ensure the preservation of a route that is free from collisions, spanning from the initial point to the final destination [7]. In their study, Li *et al.* [7] introduced an artificial fish (AFs) swarm algorithm as a means to address the navigation of mobile robots when they are in a state of wandering within their surroundings. The conversion of this path planning task into an optimization problem involves the consideration of several constraints and performance factors. Until now, there are many algorithms used for mobile robot such as ant colony algorithm proposed by Wang and Wang [8]. Miao *et al.* [9] also proposed adaptive ant colony algorithm for indoor mobile robotto overcome shortcoming of non-optimal path for the slow convergence speed. In addition, the integration of artificial immune algorithms is employed to address the challenge of 2D route planning for airplanes. The performance of this algorithm is highly influenced by the initial parameters, and a wide range of parameter values may result in reduced searchability of the algorithm. The other algorithm that contributing toward mobile robot path planning is particle swarm algorithm [10]. The particle

swarm approach requires a substantial number of samples to accurately determine the posterior probability of the system. Nevertheless, there is uncertainty regarding the legitimacy and diversity of the samples throughout the resampling phase. This circumstance has the potential to result in a reduction in sample strength, therefore rendering this technique computationally expensive [10]. While other researchers, used wheel robot to help the patient in their stroke rehabilitation with upper limb coordination program [11]. The study conducted by Bi *et al.* [12] primarily addressed the issue of binocular vision in mobile robots through the implementation of transfer learning methodologies. The authors put out a general feature extractor as a means to extract comprehensive general feature information for the purpose of domain adaptive stereo matching challenges. The utilization of robotics has been prevalent across various industries, including the hospitality sector, with the objective of enhancing the entire experience of customers. In my opinion, airports would benefit from an increased provision of personal assistance services that prioritize the secure and amicable management of guests. In response to the ongoing imperative to enhance airport security measures, the utilization of robots has been implemented in select areas to provide support to individual security personnel. Robots are currently employed in some airports to perform the task of identifying concealed weapons and other prohibited goods that are not authorized for transportation on flights. LG electronics, a company headquartered in South Korea, is currently conducting trials on a set of five airport cleaning robots and five airport guide robots with the purpose of facilitating navigation within airport premises. The airport cleaning robot is an expansive vacuum cleaner equipped with cameras, light sensors, and sensor-laden bumpers, enabling it to navigate the airport premises and effectively collect debris via the process of vacuuming. The autonomous cleaning robot possesses the capability to independently navigate and select the most optimal cleaning path by utilizing a pre-existing airport map stored within its database. Equipped with many brushes, motors, and a dust canister of substantial size, this robotic device has been specifically engineered to effectively cleanse various types of surfaces, encompassing both tiled and carpeted floors. LG claims that its robot is equipped with light detection and ranging (LIDAR) sensors, simultaneous local station, and mapping (SLAM) technology, and bumpers for obstacle detection. This combination of features enables the robot to effectively navigate through crowded airport environments while avoiding obstacles. Figure 1 shows the example of vacuum cleaner robot in Incheon Airport, South Korea.



Figure 1. LG cleaner robot in incheon Aripport, South Korea (LG electronics) [13]

In 2016, Hitachi, a Japanese technology corporation, conducted a pilot project at Tokyo's Haneda Airport including the utilization of humanoid robots, as shown in Figure 2. These robots were employed to carry out various tasks aimed at assisting passengers in navigating the airport premises. The EMIEW3 robot developed by Hitachi underwent a proof-of-concept test in September, as depicted in Figure 2. During this test, the robot was positioned on a stand in proximity to an information board located at the domestic Terminal 2 of an airport. Its functionalities included responding to inquiries, as well as presenting maps and photographs of various regions [13]. The latter phase of experimentation entailed the utilization of a robot endowed with the ability to communicate in both Japanese and English. This robot assumed the role of a guide, facilitating the navigation of travelers within Terminal 2, specifically guiding them from one location to another, such as the information boards. During the concluding stage, the robot guided guests to predetermined destinations.



Figure 2. Hitachi humanoid robot in Haneda Airport, Japan (Kyodo) [13]

Furthermore, the other researcher proposed speech recognition for residential robot using deep learning approaches [14]. The navigational tasks in robotic systems, such as autonomous vehicles (AVs), necessitate the development of environmental models and accurate system position localization within the environment. Additionally, these activities involve motion control, as well as the detection and avoidance of obstacles in highly complex environments [15]. Hence, the primary areas of concern revolve around perception, localization, motion control, and path planning [16]–[18]. The proposal put up by Lin *et al.* [19] involves the utilization of a decision tree for the purpose of field path planning. This model aims to enhance the real-time recognition of the robot's present behavior and speed, hence improving the decision-making process during its wandering. The experiment conducted demonstrates a reduction in planning time of up to 50% when compared to the typical artificial potential field (APF) technique [19]. The APF method is a well-established motion planning tool that is widely acknowledged in the field of robotics. The APF method draws heavily from the principles of potential fields in physics, thereby converting the task of path planning for robots or mobile objects into an optimization issue centered around identifying the most favorable path inside a simulated potential field. The fundamental concept revolves around perceiving the desired site as an alluring source, while regarding impediments or unfeasible areas as causes of repulsion. Obstacles are surrounded by high potential fields, whereas the goal location is surrounded by low potential fields. The APF utilizes force and direction calculations to steer the robot or item towards a path characterized by diminishing potential energy [20]. The improved method of APF in joint space is proposed by Chen *et al.* [21]. Motion planning was employed in the context of industrial robotic arm applications. This study makes two primary contributions, namely:

- A study on the implementation of AFs algorithm for path planning on autonomous navigation of mobile robots within virtual airport environments.
- The present study employs a deep learning methodology that utilizes the VGG16 pre-trained model for the purpose of stereo object matching.

2. RESEARCH METHOD

As previously said, our research endeavors revolved around enhancing the path planning capabilities of mobile robots through the utilization of AF algorithms. Additionally, we employed a deep learning strategy to enhance the process of stereo object matching by leveraging the VGG16 model, as depicted in the architecture depicted in Figure 3. The AF is a constructed organism that replicates the behavioral patterns of its natural counterpart. Typically, fish exhibit social search behavior as they relocate to a location with more consistent food availability [22]. There exist four distinct social behaviors in general: leaping behavior, swarming behavior, following behavior, and prey behavior [23], [24].

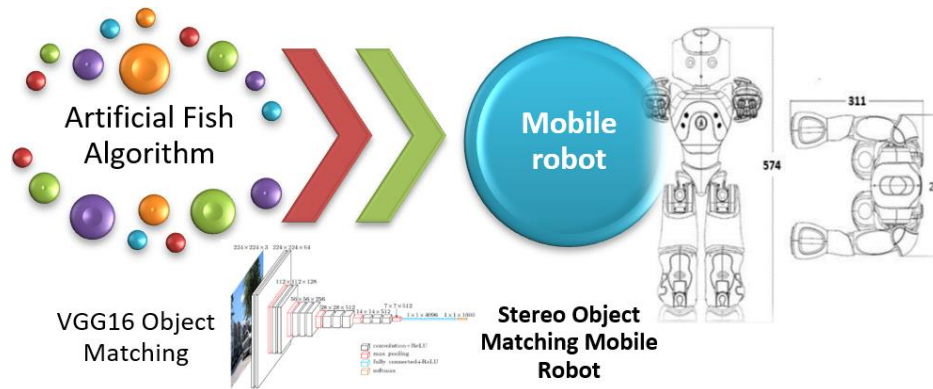


Figure 3. Proposed architecture of stereo object matching of mobile robot

2.1. AF algorithm

Assuming that an individual is denoted as vector X , it can represent the AF state. Then we can denote vector $X = (X_1, X_2, X_3, \dots, X_n)$, where $x_i (i = 1, 2, \dots, n)$ denoting optimization problem of fishes. The food concentration in the present location can be expressed as $Y = f(x)$, where Y represents the numerical value of the target function. The euclidean distance equation can be used to represent the distance between two AFs X_i and X_j as depicted in (1).

$$D_{i,j} = |x_i - x_j| \quad (1)$$

The crowd factor $\delta (0 < \delta < 1)$, the control parameters are utilized to manage the crowd around a specific point in AF. The most optimal position that AF has discovered will be stored in the post [24]. Consequently, we have elucidated the entirety of the behavior in the subsequent manner:

Prey behaviour: within the realm of natural ecosystems, the act of prey behavior serves as a fundamental biological behavior shown by fish in order to procure sustenance. The position X_j within the viewing field of the AF i might be determined arbitrarily. The variable X_i represents the present location of AF i , while X_j represents a randomly selected state of its visual distance. The food concentration, denoted as Y , can be mathematically defined as the objective function $Y = F(X)$. The position X_j can be determined through the utilization of the subsequent (2).

$$x_j = x_i + Visual \times rand(0,1) \quad (2)$$

Y_j and Y_i are utilized to ascertain the food concentration levels of X_i and X_j . In the event that Y_i is found to be less than Y_j , the autonomous agent AF proceeds to advance one step from its present location towards X_j .

This action is executed by (3).

$$X_i(t+1) = X_i(t) + \frac{X_j(t) - X_i(t)}{\|X_j(t) - X_i(t)\|} \times Step \times rand(0,1) \quad (3)$$

If Y_i is greater than Y_j , we proceed to randomly select another state, X_j , and evaluate if its food consistency meets the forward condition. When the AF i is unable to satisfy the forward requirement after a certain number of attempts, the AF in question engages in leap behavior.

Swarm behavior: to maintain swarm generality, artificial agents AFs endeavor to converge towards the central point during each iteration. The determination of the central position can be expressed mathematically by the (4).

$$X_c = \frac{1}{N} \sum_{i=1}^N X_i \quad (4)$$

The variable X_c represents the arithmetic mean of all AF swarm. The variable N represents the magnitude of the population. Let nf be the numerical value representing the quantity of AF swarming inside the optical range of X_c . If the ratio of the number of food sources found by an individual (nf) to the total number of food sources (N) is less than a certain threshold (δ), and the quality of the food source at the center position of the

swarm (Y_c) is greater than the quality of the food source at the initial location (Y_i), then the individual denoted as AF i will take a step forward towards the companion center, in contrast, AF exhibits prey behavior, as described in (5).

$$X_i(t + 1) = X_i(t) + \frac{X_c(t) - X_i(t)}{\|X_c(t) - X_i(t)\|} \times Step \times rand(0,1) \tag{5}$$

Follow behaviour: observe and analyze behavior. During the migratory phase of the AF, when an individual fish or a group of fish locate a food source, neighboring fish will promptly track and converge upon the location. Assume that the present location of the AF i is denoted as X_i , and let X_j represent a neighboring place within its viewing range. Let nf represent the quantity of AF swarming inside the visual range of X_c . If Y_i is less than Y_j and the ratio of nf to n is less than Θ , then AF i proceeds one step forward towards the neighboring X_j . In the event that there is an absence of neighboring entities X_j or if all neighboring entities express dissatisfaction with the prevailing conditions, the AF algorithm will initiate the prey behavior. The expression is denoted by (6).

$$X_i(t + 1) = X_i(t) + \frac{X_j(t) - X_i(t)}{\|X_j(t) - X_i(t)\|} \times Step \times rand(0,1) \tag{6}$$

Leap behaviour: the act of leaping is a fundamental habit shown by organisms in order to search for sustenance or social interaction across expansive territories. This behavior serves as an effective mechanism to avoid becoming trapped in suboptimal conditions. The AF identity exhibits the jump behavior by modifying the parameter to initiate a leap from its present position. The algorithm selects a state inside the visual representation and proceeds towards this state in order to circumvent the presence of local extreme values, as depicted in (7).

$$x_i(t + 1) = x_i(t) + Visual \times rand(0,1) \tag{7}$$

2.2. VGG 16 pre trained model

The VGG16 model was introduced in 2014 by Karen Simonyan and Andrew Zisserman from the Visual Geometry Group Lab at Oxford University, as documented in their work titled “Very deep convolutional networks for large-scale image recognition”. The VGG model explores the impact of layer depth using a convolutional filter size of 3x3 in order to address the challenges posed by large-scale images. The authors have published a collection of VGG models that vary in terms of the number of layers they possess. The architecture of VGG 16 is depicted in Figure 4.

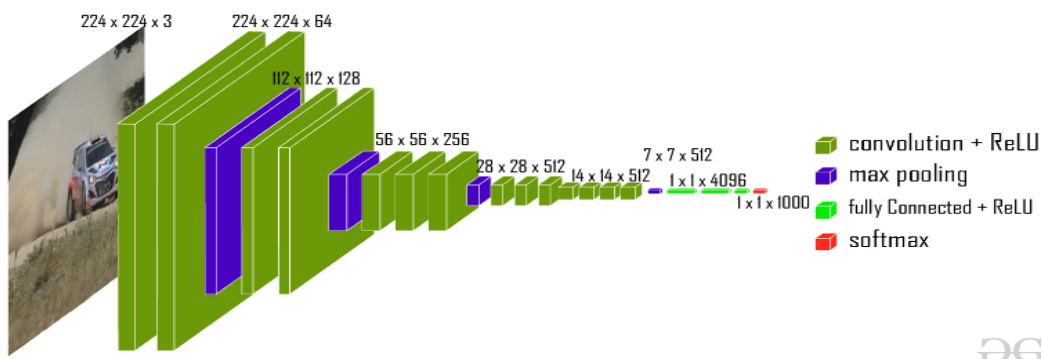


Figure 4. VGG16 architecture, image source by geeksforgeeks [25]

The concluding portion of the VGG16 network comprised of three fully linked layers, culminating in the ultimate output being acquired by the utilization of the softmax function. In (8) presents the formal representation of the softmax function in mathematics. The implication of the softmax function is that it assigns a probability value to each output classification, indicating the likelihood of belonging to each category. This contrasts with determining a single maximum value. In this context, Z_i represents the output value of the i^{th} node, and C represents the number of output nodes, which corresponds to the number of categories in the classification. The Softmax function is utilized to convert the output of many categories into a probability distribution that spans the range of [0, 1].

$$\text{Softmax}(z_i) = \frac{e^{z_i}}{\sum_{c=1}^C e^{z_c}} \quad (8)$$

3. RESULTS AND ANALYSIS

In this section, we provide into the dataset and offering an insightful explanation. We showcase the research results, which are subsequently examined thoroughly in connection with the proposed approach. These findings are then discussed comprehensively in relation to the proposed approach.

3.1. Dataset

We adopted the dataset for the mobile robot simulation from Mohammadi *et al.* [26] that have various sample of path planning. The sample of simulation track is depicted in Figure 5. While, Figure 6 is the illustration of the mobile robot movement in X-Y coordinates.

Figure 7 depicts the robot path planning design in corepgrah for our robot. The NAO robot will follow the path-planning route that was described in the preceding subsection. Nao will commence by introducing itself then proceed to navigate through the course within the building. The table provided, labeled as Table 1, displays a sample of the dataset in a tabular format. The position (Pos_i) of each robot when transitioning from one state to another is indicated by state (X_i).



Figure 5. Layout architecture of path planning simulation

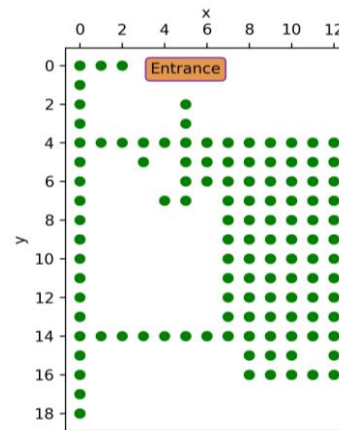


Figure 6. Layout entrance and path of robot movement

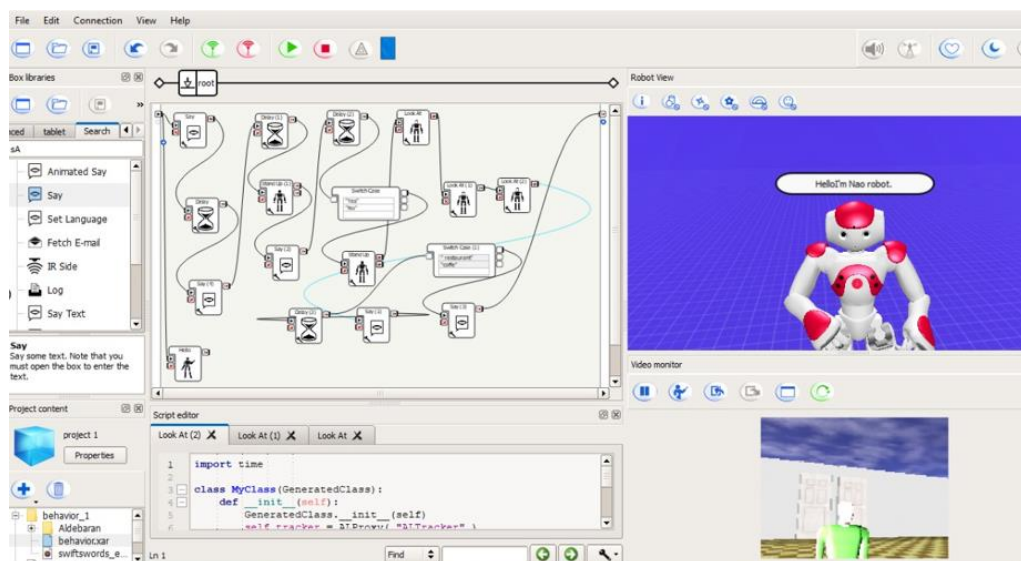


Figure 7. Robot movement simulation

Table 1. The path planning dataset

Position/State	X1	X2	X3	X4	X5	X6	X7	X8	X9	X10	X11	X12	X13
Pos1	2	2	2	0	0	0	0	0	0	0	0	0	0
Pos1	2	0	0	0	0	0	0	0	0	0	0	0	0
Pos1	2	0	0	0	0	2	0	0	0	0	0	0	0
Pos1	2	0	0	0	0	2	0	0	0	0	0	0	0
Pos1	2	2	2	2	2	2	2	2	2	2	2	2	2
Pos1	2	0	0	2	0	2	2	2	2	2	2	2	2
Pos2	2	0	0	0	0	2	2	2	2	2	2	2	2
Pos2	2	0	0	0	2	2	0	2	2	2	2	2	2
Pos2	2	0	0	0	0	0	0	2	2	2	2	2	2
Pos3	2	0	0	0	0	0	0	2	2	2	2	2	2
Pos3	2	0	0	0	0	0	0	2	2	2	2	2	2
Pos5	2	0	0	0	0	0	0	2	2	2	2	2	2
Pos6	2	0	0	0	0	0	0	2	2	2	2	2	2
Pos6	2	0	0	0	0	0	0	2	2	2	2	2	2
Pos8	2	2	2	2	2	2	2	2	2	2	2	2	2
Pos9	2	0	0	0	0	0	0	0	2	2	2	0	2
Pos10	2	0	0	0	0	0	0	0	2	2	2	2	2
Pos11	2	0	0	0	0	0	0	0	0	0	0	0	0
Pos1	2	0	0	0	0	0	0	0	0	0	0	0	0
Pos1	2	0	0	2	0	2	2	2	2	2	2	2	2
Pos2	2	0	0	0	0	2	2	2	2	2	2	2	2
Pos2	2	0	0	0	2	2	0	2	2	2	2	2	2
Pos2	2	0	0	0	0	0	0	2	2	2	2	2	2
Pos3	2	0	0	0	0	0	0	2	2	2	2	2	2
Pos3	2	0	0	0	0	0	0	2	2	2	2	2	2
Pos5	2	0	0	0	0	0	0	2	2	2	2	2	2
Pos6	2	0	0	0	0	0	0	2	2	2	2	2	2
Pos7	2	0	0	0	0	0	0	2	2	2	2	2	2

Figure 8 is a heatmap diagram illustrating the robot’s trajectory as it moves from one position to another during the simulation by using AFs. Position 1 exhibits superiority over other positions, as it is frequently visited by robots. This behavior exemplifies the prey behavior in the AFs algorithm. Pos8 indicates the subsequent behavior of the AFs algorithm. Robots occasionally return to their original position while manoeuvring to avoid obstacles or when attempting to locate the correct path.

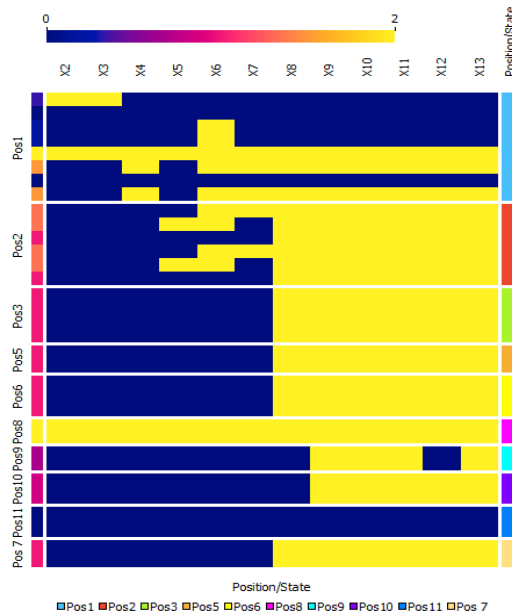


Figure 8. Heat map of the robot motion simulation

3.2. Stereo object matching

As the robot explores its surroundings, it has the ability to detect and locate a wide range of items in its vicinity. This object can either be hazardous or a common item utilized by humans in their daily routines.

We employed AdaBoost, Naïve Bayes, and random forest as classifiers for object recognition. We focused on explaining Adaboost step as follows due to its acquired highest score in testing:

- At first, each instance is assigned an equal weight of $w(i)=(1/m)$, where m is the total number of instances.
- The initial base learner will be constructed by employing decision tree stumps within the AdaBoost algorithm. Decision stumps are essentially decision trees with a maximum depth of 1, consisting of a single decision node and two leaf nodes.
- Upon completing the training of the initial base learner, the weighted error, denoted as $r(j)$, will be calculated for any misclassified or poorly fitting class based on the predictions made by the first base learner ($y(observer) \neq y(predicted)$). The formula for error rate is as (9).

$$r_j = \frac{\sum_{i=1}^m \omega^{(i)} \mathbb{1}_{\hat{y}_j^{(i)} \neq y^{(i)}}}{\sum_{i=1}^m \omega^{(i)}} \text{ Where } \hat{y}_j^{(i)} \text{ is the } j^{\text{th}} \text{ predictor's prediction for the } i^{\text{th}} \text{ instance} \quad (9)$$

- The weight of the predictor will be calculated using the following method in order to observe the performance of the choice, as described in (10);

$$\alpha_j = \eta \log \frac{1-r_j}{r_j} \quad (10)$$

where η is the learning rate hyperparameter, which has a default value of 1. It influences the importance assigned to weak learners in the final forecast of the ensemble. The greater the accuracy of the prediction, the more weight will be attributed to it.

- In the process of data change, the weights will be updated and increased exponentially for the mistakenly anticipated events, while they will be dropped for the successfully predicted cases, as described in (11), then all instance weigh is normalized.

$$\begin{aligned} & \text{for } i = 1, 2, \dots, m \\ \omega^{(i)} & \leftarrow \begin{cases} \omega^{(i)} \exp(\alpha_j) & \text{if } \hat{y}_j^{(i)} = y^{(i)} \\ \omega^{(i)} \exp(-\alpha_j) & \text{if } \hat{y}_j^{(i)} \neq y^{(i)} \end{cases} \end{aligned} \quad (11)$$

- In order to create the final prediction, AdaBoost algorithm utilizes the weights α assigned to each predictor to calculate and assign weights to the predictions made by all the base learners. The final predicted class will be the one that receives the majority of the weighted votes, refer to (12).

$$\hat{y}(X) = \underset{\hat{y}(X)=k}{\operatorname{argmax}} \sum_{j=1}^N \alpha_j, \text{ where } N \text{ is the number of predictors} \quad (12)$$

We have provided two items, specifically a pistol and a lighter, for the purpose of identifying objects. Figures 9 and 10 portray these things, respectively. The recognition technique exhibits significant potential, with an accuracy rate of 84.7% for identifying guns and 84.15% for identifying individuals. Despite being held by hand and having some of its parts obstructed, the lighter achieved an accuracy of 84.21%. AdaBoost achieves an accuracy of 92%, whilst Naïve Bayes and random forest fall short with scores below AdaBoost at 89%, as described in Figure 11.



Figure 9. Gun object

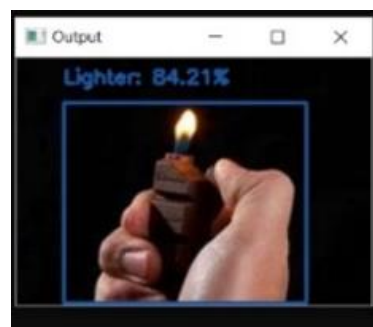


Figure 10. Lighter object

Model	AUC	CA	F1	Prec	Recall	MCC
AdaBoost	0.924	0.929	0.800	1.000	0.667	0.782
Naive Bayes	0.894	0.929	0.800	1.000	0.667	0.782
Random Forest	0.894	0.857	0.667	0.667	0.667	0.576

Figure 11. Score comparison between three classifiers

Figure 12 displays the ROC curve for the three classifiers. It is evident that AdaBoost has exhibited a substantial increase since the start of the curve, followed by the other two classifiers. The curves of three classifiers intersect at the points 0.102 and 0.354. Subsequently, with a score of 0.500, the AdaBoost classifier has already surpassed the other two classifiers.

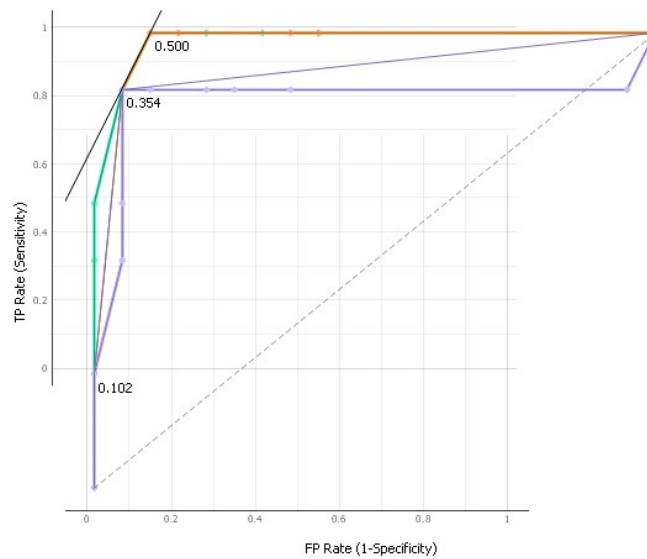


Figure 12. ROC curve score for object recognition

4. CONCLUSION

The prevalence of robots is increasing, not only in industrial settings but also in everyday locations like airports. Lately, numerous entities have conducted trials using robots designed to enhance airport cleanliness and safety and the overall passenger experience. The path planning for mobile robots using the AFs algorithm showed excellent results. The robot can imitate the prey behaviour of the AFs algorithm, as shown by the dominance of pos one during the simulation. The other behaviour that is demonstrated by our robot is the following behaviour. This behaviour is affected by food sources in the AFs algorithm. At the same time, mobile robot is affected by stimulation of their neighbouring response. Subsequently, the three main classifiers are used for stereo-object matching for various objects. The recognition rate is relatively high and promising, with a 92.4% accuracy rate performed by the AdaBoost classifier. This outcome is promising for enhancing the path planning of mobile robots that have vision surveillance toward their environment.

ACKNOWLEDGEMENTS

This work was supported by the deanship of scientific research (DSR), King Abdulaziz University, Jeddah Saudi Arabia. Therefore, gratefully acknowledge the DSR technical and financial support.

REFERENCES




[1] A. H. Basori, "NAO-Teach: helping kids to learn societal and theoretical knowledge with friendly human-robot interaction," *Indonesian Journal of Electrical Engineering and Computer Science*, vol. 17, no. 3, pp. 1657–1664, 2020, doi: 10.11591/IJEECS.V17.I3.PP1657-1664.

[2] C. Deng, D. Liu, H. Zhang, J. Li, and B. Shi, "Semi-global stereo matching algorithm based on multi-scale information fusion," *Applied Sciences (Switzerland)*, vol. 13, no. 2, 2023, doi: 10.3390/app13021027.

- [3] T. H. Huynh and M. Yoo, "A taillight matching and pairing algorithm for stereo-vision-based nighttime vehicle-to-vehicle positioning," *Applied Sciences (Switzerland)*, vol. 10, no. 19, 2020, doi: 10.3390/app10196800.
- [4] P. Liu, L. Zhang, and M. Wang, "Measurement of large-sized-pipe diameter based on stereo vision," *Applied Sciences (Switzerland)*, vol. 12, no. 10, 2022, doi: 10.3390/app12105277.
- [5] H. Shalma and P. Selvaraj, "A review on 3D image reconstruction on specific and generic objects," *Materials Today: Proceedings*, vol. 80, pp. 2400–2405, 2023, doi: 10.1016/j.matpr.2021.06.371.
- [6] S. Zhou, G. Zhang, R. Yi, and Z. Xie, "Research on vehicle adaptive real-time positioning based on binocular vision," *IEEE Intelligent Transportation Systems Magazine*, vol. 14, no. 4, pp. 47–59, 2022, doi: 10.1109/MITS.2021.3049422.
- [7] F. F. Li, Y. Du, and K. J. Jia, "Path planning and smoothing of mobile robot based on improved artificial fish swarm algorithm," *Scientific Reports*, vol. 12, no. 1, 2022, doi: 10.1038/s41598-021-04506-y.
- [8] Q. Wang and Y. Wang, "Route planning based on combination of artificial immune algorithm and ant colony algorithm," *Advances in Intelligent and Soft Computing*, vol. 122, pp. 121–130, 2011, doi: 10.1007/978-3-642-25664-6_16.
- [9] C. Miao, G. Chen, C. Yan, and Y. Wu, "Path planning optimization of indoor mobile robot based on adaptive ant colony algorithm," *Computers and Industrial Engineering*, vol. 156, 2021, doi: 10.1016/j.cie.2021.107230.
- [10] M. Neshat, A. A. Pourahmad, and Z. Rohani, "Improving the cooperation of fuzzy simplified memory A* search and particle swarm optimisation for path planning," *International Journal of Swarm Intelligence*, vol. 5, no. 1, p. 1, 2020, doi: 10.1504/ijsi.2020.106388.
- [11] A. H. Basori, "End-effector wheeled robotic arm gaming prototype for upper limb coordination control in home-based therapy," *Telkomnika (Telecommunication Computing Electronics and Control)*, vol. 18, no. 4, pp. 2080–2086, 2020, doi: 10.12928/TELKOMNIKA.V18I4.3775.
- [12] Y. Bi, C. Li, X. Tong, G. Wang, and H. Sun, "An application of stereo matching algorithm based on transfer learning on robots in multiple scenes," *Scientific Reports*, vol. 13, no. 1, 2023, doi: 10.1038/s41598-023-39964-z.
- [13] B. Read, "Rise of the airport robots," *Royal Aeronautic Society*, 2017. <https://www.aerosociety.com/news/rise-of-the-airport-robots/> (accessed Aug. 01, 2023).
- [14] R. Jiménez-Moreno and R. A. Castillo, "Deep learning speech recognition for residential assistant robot," *IAES International Journal of Artificial Intelligence*, vol. 12, no. 2, pp. 585–592, 2023, doi: 10.11591/ijai.v12.i2.pp585-592.
- [15] K. Karur, N. Sharma, C. Dharmatti, and J. E. Siegel, "A survey of path planning algorithms for mobile robots," *Vehicles*, vol. 3, no. 3, pp. 448–468, 2021, doi: 10.3390/vehicles3030027.
- [16] C. Zheng and R. Green, "Vision-based autonomous navigation in indoor environments," *International Conference Image and Vision Computing New Zealand*, 2010, doi: 10.1109/IVCNZ.2010.6148876.
- [17] N. Sariff and N. Buniyamin, "An overview of autonomous mobile robot path planning algorithms," *SCORED 2006 - Proceedings of 2006 4th Student Conference on Research and Development "Towards Enhancing Research Excellence in the Region"*, pp. 183–188, 2006, doi: 10.1109/SCORED.2006.4339335.
- [18] N. B. Sariff and N. Buniyamin, "Ant colony system for robot path planning in global static environment," in *International conference on System Science and Simulation in Engineering - Proceedings*, 2010, pp. 192–197.
- [19] X. Lin, Z. Q. Wang, and X. Y. Chen, "Path planning with improved artificial potential field method based on decision tree," *27th Saint Petersburg International Conference on Integrated Navigation Systems, ICINS 2020 - Proceedings*, 2020, doi: 10.23919/ICINS43215.2020.9134006.
- [20] O. Khatib, "Real-time obstacle avoidance for manipulators and mobile robots," *Proceedings - IEEE International Conference on Robotics and Automation*, pp. 500–505, 1985, doi: 10.1109/ROBOT.1985.1087247.
- [21] Y. Chen, L. Chen, J. Ding, and Y. Liu, "Research on real-time obstacle avoidance motion planning of industrial robotic arm based on artificial potential field method in joint space," *Applied Sciences (Switzerland)*, vol. 13, no. 12, 2023, doi: 10.3390/app13126973.
- [22] R. Azizi, "Empirical study of artificial fish swarm algorithm," 2014, [Online]. Available: <http://arxiv.org/abs/1405.4138>.
- [23] Y. Gao, L. Guan, and T. Wang, "Triaxial accelerometer error coefficients identification with a novel artificial fish swarm algorithm," *Journal of Sensors*, vol. 2015, 2015, doi: 10.1155/2015/509143.
- [24] Y. Zhang, G. Guan, and X. Pu, "The robot path planning based on improved artificial fish swarm algorithm," *Mathematical Problems in Engineering*, vol. 2016, 2016, doi: 10.1155/2016/3297585.
- [25] Pawangfg, "VGG-16 | CNN model," *Geeksforgeeks*, 2023. <https://www.geeksforgeeks.org/vgg-16-cnn-model/> (accessed Aug. 01, 2023).
- [26] M. Mohammadi, A. Al-Fuqaha, and J. S. Oh, "Path planning in support of smart mobility applications using generative adversarial networks," *Proceedings - IEEE 2018 International Congress on Cybermatics: 2018 IEEE Conferences on Internet of Things, Green Computing and Communications, Cyber, Physical and Social Computing, Smart Data, Blockchain, Computer and Information Technology, iThings/GreenCom/CPSCoM/SmartData/Blockchain/CIT 2018*, pp. 878–885, 2018, doi: 10.1109/Cybermatics_2018.2018.00168.

BIOGRAPHIES OF AUTHORS



Andi Besse Firdausiah Mansur    received B.Sc. (Mathematics), in 2004 and M.Sc. (Software Engineering) in 2009. Furthermore, she obtained Ph.D. degree in Software Engineering from Universiti Teknologi Malaysia, Johor Bahru, Johor, in 2013. From 2013 to present, she is assistant professor at Faculty of Computing and Information Technology Rabigh, King Abdulaziz University. She is member of reviewer board in some international journal. Her research interest: social network analysis, e-learning, computer vision, robotics, artificial intelligence, data mining, and mathematics. She can be contacted at email: abmansur@kau.edu.sa.